Zoological Studies **61**:22 (2022)
doi:10.6620/ZS.2022.61-22

Zoological Studies

Open Access

Macrobiotus naginae sp. nov., a New Xerophilous Tardigrade Species from Rokua Sand Dunes (Finland)

Matteo Vecchi[1,*], Daniel Stec[2,3], Tommi Vuori[1], Serge Ryndov[1], Justine Chartrain[1], and Sara Calhim[1]

[1]*Department of Biological and Environmental Science, University of Jyvaskyla, PO Box 35, FI-40014 Jyvaskyla, Finland.*
**Correspondence: E-mail: matteo.vecchi15@gmail.com (Vecchi).*
E-mail: tommi.o.vuori@student.jyu.fi (Vuori); reraom7@gmail.com (Ryndov); justine.j.chartrain@jyu.fi (Chartrain); sara.calhim@jyu.fi (Calhim)
[2]*Institute of Systematics and Evolution of Animals, Polish Academy of Sciences, Sławkowska 17, 31-016 Kraków, Poland.*
E-mail: daniel.stec@isez.pan.krakow.pl (Stec)
[3]*Institute of Zoology and Biomedical Research, Faculty of Biology, Jagiellonian University, Gronostajowa 9, 30-387 Kraków, Poland.*

Received 19 November 2021 / Accepted 11 March 2022 / Published 30 May 2022
Communicated by Benny K.K. Chan

Animals that colonize soil show specific adaptations to soil. Compared to closely related species living on the surface, the limbs of soil-dwelling animals are often shortened, reduced, or absent to allow a less restricted passage through cavities between soil particles. This pattern of limb reduction has also been observed in tardigrades, where multiple lineages that colonized the below-ground habitat show independent reduction and/or loss of legs and claws. In the tardigrade superfamily Macrobiotoidea, leg and claw reductions are a common trait found in the *Macrobiotus pseudohufelandi* complex. This rarely found species complex currently contains four nominal taxa. Here we describe, with the use of integrative taxonomy, *Macrobiotus naginae* sp. nov., a new species in the *Macrobiotus pseudohufelandi* complex from inland sand dunes in Finland. We also provide a dichotomous key to the *Macrobiotus pseudohufelandi* complex to assist with their identification in future studies.

Key words: Tardigrada, *Macrobiotus pseudohufelandi* complex, Sand dunes, Taxonomy, Systematics, Soil habitat.

BACKGROUND

Animals that live in the soil have specific adaptations. Animal species living underground in the soil show shortened, reduced, or absent limbs compared to closely related species living on the surface to allow a less restricted passage through cavities between soil particles (Villani et al. 1999). This pattern of limb reduction has also been observed in tardigrades, where multiple lineages that have colonized the below-ground habitat show independent reduction and/or loss of legs and claws (Bertolani and Biserov 1996). Tolerance to desiccation is also an important adaptation when living in soil habitats with reduced amount of water (Roszkowska et al. 2021). In the tardigrade superfamily Macrobiotoidea, leg and claw reductions are found in the *Macrobiotus pseudohufelandi* complex as well as in the genus *Pseudohexapodibius* Bertolani & Biserov, 1996. The first two members of the *Macrobiotus pseudohufelandi* complex were described as *Macrobiotus pseudohufelandi* Iharos, 1966 and *Parhexapodibius xerophilus* Dastych, 1978. Later, Bertolani and Biserov (1996) recognized the similarities in their buccal apparatus and in the claw symmetry and erected for those two species the easily recognizable genus *Xerobiotus*. The third formally described species, *Macrobiotus euxinus* (Pilato, Kiosya, Lisi, Inshina & Biserov, 2011), was found in Ukraine and it is

Citation: Vecchi M, Stec D, Vuori T, Ryndov S, Chartrain J, Calhim S. 2022. *Macrobiotus naginae* sp. nov., a new xerophilous tardigrade species from Rokua sand dunes (Finland). Zool Stud **61**:22. doi:10.6620/ZS.2022.61-22.

most similar to *Macrobiotus pseudohufelandi*, from which it differs mainly by morphometric characters. The fourth and last described species, *Macrobiotus gretae* (Massa, Guidetti, Cesari, Rebecchi & Jönsson, 2021), was found in Sweden; however, molecular data confirmed its presence also in South Africa (Massa et al. 2021). Phylogenetic analyses showed that taxa previously recognized as *Xerobiotus* are deeply nested inside the genus *Macrobiotus* (Stec et al. 2020a 2021; Kiosya et al. 2021; Vecchi and Stec 2021; Stec et al. in press). Except for the specific adaptations to life in soil (reduced legs and claws), *Xerobiotus* taxa share with *Macrobiotus* the following characters: the presence of cuticular pores, identical buccal apparatus structure as well as similar sperm and egg morphology (Rebecchi 1997; Stec et al. 2021). In addition, in order for tardigrade taxonomy to reflect evolutionary relationships in the phylum, Stec et al. (2021) abolished the genus *Xerobiotus* and transferred its species to *Macrobiotus*, creating a species complex for them. Supressing *Xerobiotus* preserves the monophyly of *Macrobiotus* and expands the diagnostic features of *Macrobiotus* to encompass the *Xerobiotus* morphotype. Species of the *Macrobiotus pseudohufelandi* complex are usually found in uncommon substrates such as mosses growing on sandy soils or dunes. The scarcity of material (especially eggs) available for each description has led to a poor understanding of the actual species and morphological diversity in this peculiar tardigrade group. To further contribute to our understanding of the *M. pseudohufelandi* complex, here we describe a new species from sand dunes in inland Finland.

MATERIALS AND METHODS

Study area

Rokua National Park is located in the North Ostrobothnia region of Finland. As one of their northernmost locations in Finland, it is a key habitat for rare and threatened esker (long, winding ridge of stratified sand and gravel) organisms (Sarala et al. 2006), including many plant species adapted to parched environments (*e.g.*, *Carex ericetorum*, *Thymus serpyllum serpyllum* and *Pilosella peleteriana*, Jalas, 1953), which in turn support many lepidopteran and hymenopteran taxa (From 2005). However, Rokua's main feature is the presence of aeolian deposits that take the form of not only eskers, but also inland sand dunes (composed by medium-fine sand with grains size 0.03–1.50 mm), kettle holes (depression in a plain formed by retreating glaciers or draining floodwaters) and kames (irregularly shaped hill or mound composed of sand, gravel and till that accumulates in a depression on a retreating glacier) (Aartolahti 1973). The dominant vegetation cover in these formations is a lichen-rich forest, composed mainly of *Cladonia*, and to a lesser extent, *Vaccinium* and *Calluna* lichens; only a few patches of moss (*Polytrichum*, *Pleurozium* and *Dicranum*) co-occur (Aartolahti 1973). Finnish inland dune forests are a delicate habitat that is threatened on many fronts, chief among them being human activity and lack of forest fires (Kontula and Raunio 2018).

Samples and specimens

Samples of mosses, lichens, leaf litter and grass roots on different substrates (mostly on sand) were collected from Rokua National Park (Finland) on the 25th of May 2020 by M.V., J.C., S.R., and S.C. See table 1 for the sample coordinates and additional tardigrade genera found. The samples were examined for tardigrades using the sieving protocol by Dastych (1980) and the N-G Baermann extractor protocol by Czerneková et al. (2018). To perform the taxonomic analysis, animals and eggs were split into several groups for specific analyses: morphological analysis with PCM and SEM, as well as DNA sequencing (for details see Table 1).

Microscopy and imaging

Specimens for light microscopy were mounted on microscope slides in a small drop of Hoyer's medium and secured with a cover slip, following the protocol by Morek et al. (2016). Slides were examined under an Olympus BX53 light microscope with phase contrast (PCM), associated with an Olympus DP74 digital camera. To obtain clean and extended specimens for SEM, tardigrades were processed according to the protocol by Stec et al. (2015). Additional specimens (n = 2) were stained with Orcein (see Bertolani 1971) and examined for the presence of sperm. Specimens were examined under high vacuum in a Raith e-LINE E-beam at the Nanoscience Center of Jyväskylä University, Finland. All figures were assembled in FigureJ (Mutterer and Zinck 2013). For structures that could not be satisfactorily focused in a single light microscope photograph, a stack of 2–6 images was taken with an equidistance of ca. 0.2 µm and assembled manually into a single deep-focus image in Corel Photo-Paint X6. Photographs of *Macrobiotus* gr. *pseudohufelandi* PL.360 and *Macrobiotus gretae* ZA.373 (Stec et al. 2021) claws IV were kindly provided by Witold Morek (Jagellonian University, Poland).

Morphometrics and morphological nomenclature

All measurements are given in micrometres (μm). Sample size was adjusted following recommendations by Stec et al. (2016). Structures were measured only if their orientation was suitable. Body length was measured from the anterior extremity to the end of the body, excluding the hind legs. The terminology used to describe oral cavity armature and eggshell morphology follows Michalczyk and Kaczmarek (2003) and Kaczmarek and Michalczyk (2017). Macroplacoids length sequence is given according to Kaczmarek et al. (2014). Buccal tube length and the level of the stylet support insertion point were measured according to Pilato (1981). The *pt* index is the ratio of the length of a given structure to the length of the buccal tube (Pilato 1981). Measurements of buccal tube widths, heights of claws and eggs follow Kaczmarek and Michalczyk (2017). Morphometric data were handled using the "Parachela" ver. 1.7 template available from the Tardigrada Register (Michalczyk and Kaczmarek 2013). The raw morphometric data are provided as the supplementary materials (Table S1). Tardigrade taxonomy follows Bertolani et al. (2014) and Stec et al. (2021).

Genotyping

The DNA was extracted from individual animals following a Chelex® 100 resin (BioRad) extraction method by Casquet et al. (2012) with modifications described in detail in Stec et al. (2020b). Each specimen was mounted in water and examined under a light microscope to verify the identification prior to DNA extraction. We sequenced four DNA fragments, three nuclear (18S rRNA, 28S rRNA, ITS2) and one mitochondrial (*COI*). All fragments were amplified and sequenced according to the protocols described in Stec et al. (2020b); primers with original references are listed in table 2. Sequencing products were read with the ABI 3130xl sequencer in the Molecular Ecology Lab, Institute of Environmental Sciences of the Jagiellonian University, Kraków, Poland. Sequences were processed in MEGA7 (Kumar et al. 2016) and submitted to NCBI GenBank (Table 3).

Phylogenetic analysis

The phylogenetic analyses were conducted using concatenated 18S rRNA + 28S rRNA + ITS–2 + *COI* sequences. All Macrobiotidae isolates/strains with the 4 sequenced markers present in GenBank were included

Table 1. Analysed samples containing *Macrobiotus naginae* sp. nov. Square brackets indicate the number of analysed specimens [animals + eggs]. All sampling sites are at about 60 m a.s.l.

Sample code	Coordinates	*Macrobiotus naginae* sp. nov. material analysed	Substrate	Other taxa found
S226	64°34'36.4"N 26°29'46.1"E	PCM (Holotype + Paratypes) [6+2] + SEM [11+3] + Orcein [2+0] + DNA [2+0]	Moss on sand	
S227	64°35'06.3"N 26°30'45.0"E	PCM (Paratypes) [18+5]	Moss on sand	
S228	64°35'06.5"N 26°30'46.6"E	PCM (Paratypes) [1+0]	Moss on sand	*Milnesium*
S232	64°34'30.3"N 26°31'34.5"E	PCM (Paratypes) [2+0]	Moss on sand	*Macrobiotus*
S233	64°34'28.8"N 26°31'31.7"E	PCM (Paratypes) [2+0]	Moss and lichen on sand	*Macrobiotus*
S235	64°34'27.5"N 26°31'38.3"E	PCM (Paratypes) [2+0]	Moss on sand	
S245	64°34'26.2"N 26°31'38.5"E	PCM (Paratypes) [5+0]	Moss and lichen on sand	*Minibiotus*
S246	64°34'41.1"N 26°31'09.9"E	PCM (Paratypes) [6+0]	Lichen on sand	
S247	64°34'41.2"N 26°31'10.1"E	PCM (Paratypes) [8+0]	Moss on sand	
S248	64°34'44.9"N 26°31'07.0"E	PCM (Paratypes) [10+0]	Lichen on sand	
S249	64°34'46.3"N 26°31'06.5"E	PCM (Paratypes) [9+0]	Moss and lichen on sand	

in the analysis. In addition, all sequences from members of *Macrobiotus* clade B (*sensu* Stec et al. 2021) were included. Sequences from Adorybiotidae, Murrayidae and Richtersiusidae were used as outgroups. Additional Macrobiotidae populations were sequenced for the four markers to improve the phylogenetic reconstruction (in Table S2). GenBank accession numbers of the newly generated sequences are presented in table 2. Accession numbers of sequences downloaded from GenBank are listed in table S3.

The sequences of the 18S and 28S markers did not completely overlap (thus creating problems in the alignment phase), so they had to be aligned to reference alignments. The reference alignments were generated by downloading the longest available sequences for tardigrades on GenBank and aligned using MAFFT ver. 7 (Katoh et al. 2002; Katoh and Toh 2008) with the G-INS-i method (thread = 4, threadtb = 5, threadit = 0, reorder, adjust direction, any symbol, max iterate = 1000, retree 1, global pair input). Reference alignments are available as appendixes 1 and 2.

The sequences to be analysed were then aligned to the corresponding reference alignment using MAFFT ver. 7 with the L-INS-i method (thread = 8, adjustdirection, ep = 0.0, add new_sequences, localpair, maxiterate = 16). The ITS-2 sequences were aligned using MAFFT ver. 7 (Katoh et al. 2002; Katoh and Toh 2008) with the G-INS-i method (thread = 4, threadtb = 5, threadit = 0, reorder, adjust direction, any symbol, max iterate=1000, retree = 1, global pair input). The *COI* sequences were aligned according to their amino acid sequences (translated using the invertebrate mitochondrial code) with the MUSCLE algorithm (Edgar 2004) in MEGA7 with default settings (all gap penalties = 0, max iterations = 8, clustering method = UPGMB, lambda = 24). Alignments were visually inspected and trimmed in MEGA7. Sequences were concatenated with the R package 'concatipede' v1.0.0 (Vecchi and Bruneaux 2021).

Model selection was performed for each alignment partition (6 in total: 18S rRNA, 28S rRNA, ITS-2 and three *COI* codons) with PartitionFinder2 (Lanfear

Table 2. Primers with their original references used for amplification of the four DNA fragments sequenced in the study

DNA marker	Primer name	Primer direction	Primer sequence (5'-3')	Primer source
18S rRNA	18S_Tar_Ff1	forward	AGGCGAAACCGCGAATGGCTC	Stec et al. (2017)
	18S_Tar_Rr1	reverse	GCCGCAGGCTCCACTCCTGG	
28S rRNA	28S_Eutar_F	forward	ACCCGCTGAACTTAAGCATAT	Gąsiorek et al. (2018) Mironov et al. (2012)
	28SR0990	reverse	CCTTGGTCCGTGTTTCAAGAC	
ITS-2	ITS2_Eutar_Ff	forward	CGTAACGTGAATTGCAGGAC	Stec et al. (2018)
	ITS2_Eutar_Rr	reverse	TCCTCCGCTTATTGATATGC	
COI	LCO1490-JJ	forward	CHACWAAYCATAAAGATATYGG	Astrin and Stüben (2008)
	HCO2198-JJ	reverse	AWACTTCVGGRTGVCCAAARAATCA	

Table 3. Newly generated sequences GenBank accession numbers

	18S	28S	*COI*	ITS2
Macrobiotus naginae sp. nov. S226-01	OK663219	OK663230	OK662990	OK663209
Macrobiotus naginae sp. nov. S226-02	OK663220	OK663231	OK662991	OK663208
Macrobiotus hufelandi S605-1	OK663221	OK663232	OK662992	OK663210
Macrobiotus hufelandi S605-2	OK663222	OK663233	OK662993	OK663211
Macrobiotus sandrae S859-1	OK663223	OK663234	OK662994	OK663212
Macrobiotus cf. *sapiens* S12-1	OK663226	OK663237	OK662997	OK663215
Macrobiotus scoticus DK.056-1	OK663218	OK663228	OK662989	OK663207
Macrobiotus scoticus DK.056-2	OK663217	OK663229	OK662988	OK663206
Minibiotus cf. *diversus* S69-1	OK663227	OK663238	*	OK663216
Paramacrobiotus richtersi S38-1	OK663224	OK663235	OK662995	OK663213
Paramacrobiotus spatialis S107-1	OK663225	OK663236	OK662996	OK663214

Notes: * See table S3.

et al. 2016), partitions and models selection process and results are present in appendix 3. BI phylogenetic reconstruction was done with MrBayes v3.2.6 (Ronquist et al. 2012) without BEAGLE on the CIPRES Science Gateway (Miller et al. 2010).

Two runs with one cold chain and three heated chains were run for 25 million generations with a burning of 2.5 million generations, sampling a tree every 1000 generations. Posterior distribution sanity was checked with the Tracer v1.7 (Rambaut et al. 2018). MrBayes input file with the input alignment is available as appendix 4. The phylogenetic tree was visualized with FigTree v1.4.4 (Rambaut 2007) and the image was edited with Inkscape 0.92.3 (Bah 2011). The complete phylogenetic tree is available in appendix 5.

Species delimitation

Only a subset of the *COI* alignment containing the species of the *Macrobiotus pseudohufelandi* complex + *Mac. annewintersae* + *Mac. polonicus* AT.002 was used for species delimitation, which was performed on the K80 distance matrix of the alignment with the ABGD online server (Puillandre et al. 2012) with default parameters (Pmin = 0.001, Pmax = 0.1, Steps = 10, X = 1.5, TS/TV = 2.0, Nb bins = 20). Results are available as appendix 6.

RESULTS

Species delimitation and phylogenetic reconstruction

The phylogenetic reconstruction (Fig. 1) recovered the same overall topology of Stec et al. (2021), with the genus *Macrobiotus* and its three clades (A, B and C) being monophyletic. However, the relationships

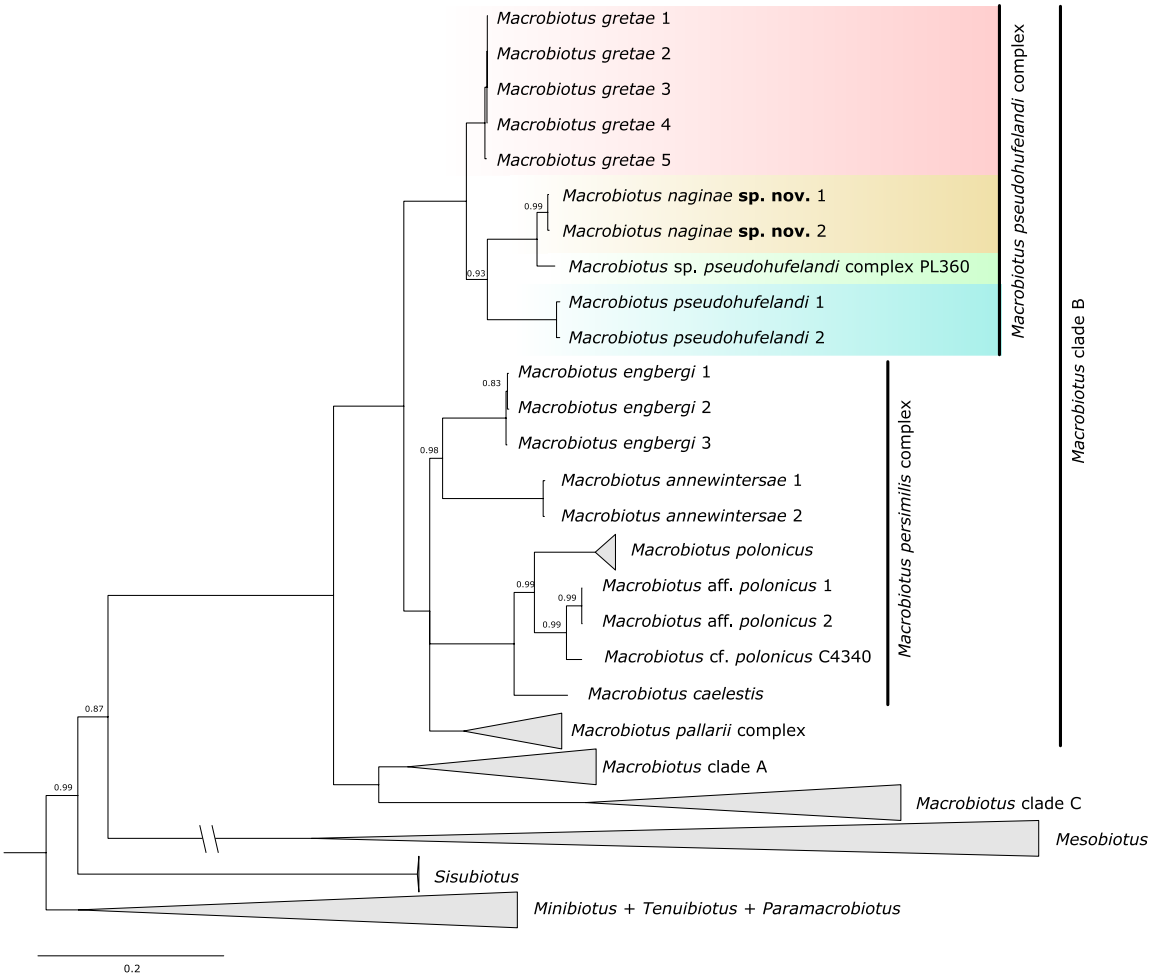

Fig. 1. Phylogenetic reconstruction of Macrobiotidae based on four concatenated markers (18S + 28S + *COI* + ITS2). Boxes delimit species of the *Macrobiotus pseudohufelandi* complex identified by ABGD performed on the *COI* alignment. Outgroups not shown. Values above branches represent node posterior probabilities (pp). pp = 1 not shown. All nodes with pp < 0.70 were collapsed.

between these three clades are different from Stec et al. (2021) as clade A and C are in a sister relationship. In addition, the *persimilis* complex was not recovered to be monophyletic. The *pseudohufelandi* group is confirmed to be nested inside *Macrobiotus* and basal in clade B.

The ABGD species delimitation recovered the presence of four species among all the *Macrobiotus pseudohufelandi* complex sequences used (Fig. 1). Those species form a well-supported (posterior probability (pp) = 1, Fig. 1) monophyletic group with respect to the outgroups. *Macrobiotus gretae* appears have a sister relationship with a clade comprising all other species. The two newly sequenced individuals from Finland are most closely related to an unidentified species from Poland (*Macrobiotus* sp. *pseudohufelandi* complex PL.360).

TAXONOMIC ACCOUNT

Phylum: Tardigrada Doyère, 1840
Class: Eutardigrada Richters, 1926
Order: Parachela Schuster, Nelson, Grigarick and Christenberry, 1980
Superfamily: Macrobiotoidea Thulin, 1928 (in Marley et al. 2011)
Family: Macrobiotidae Thulin, 1928
Genus: *Macrobiotus* Schultze C.A.S., 1834

Macrobiotus naginae sp. nov. Vecchi, Stec, Vuori, Ryndov, Chartrain and Calhim

(Figs. 2–6; Tables 4–5; Table S1)
urn:lsid:zoobank.org:act:53E10ACB-6DAA-4E63-B263-5919B00FDF3C

Material examined: 47 animals and 10 eggs. Specimens mounted on microscope slides in Hoyer's medium (34 animals + 7 eggs), fixed on SEM stubs (11 + 3), and processed for DNA sequencing (2+0).

Type locality: 64°34'36.4"N 26°29'46.1"E; 37 m a.s.l.; Rokua National Park, Utajärvi, Finland; moss on sand; coll. 25th of May 2020 by Matteo Vecchi, Sara Calhim, Justine Chartrain and Serge Ryndov.

Type repository: Holotype (S226.SL1.F with 5 paratypes), 74 paratypes (slides S227.SL1, S228.SL1, S232.SL1, S233.SL1, S235.SL1, S245.SL1, S246.SL1, S247.SL1, S248.SL1, S249.SL1; SEM stubs S226-1t) and 12 eggs (slides S226.SL.2–3, S227.SL.2–4; SEM stub S226-e1) are deposited at the Department of Biological and Environmental Sciences, University of Jyväskylä (Survontie 9C, 40500, Jyväskylä, Finland).

Etymology: Named after J. K. Rowling's Harry Potter book series character Nagini – Lord Voldemort's treasured snake companion. Formerly a cursed woman who is ultimately and irreversibly transformed into a limbless beast, this fictional character provides a fitting name for the new species in the *pseudohufelandi* complex, which in turn is characterized by reduced legs and claws.

Species description: *Animals (measurements and statistics in Table 4)*: In live animals, body opaque whitish; transparent after fixation in Hoyer's medium (Fig. 2A). Eyes present in live animals and after fixation in Hoyer's medium. Cuticular pores weakly visible in PCM, and very visible in SEM (Figs. 2B–C, 3A–B) present on the dorsal surface of body and legs. Under PCM no granulation visible on legs. Few pores present on legs (Fig. 3A–B). Garter-like structure (as defined by Massa et al. 2021) covered with microgranulation present on all legs (Fig. 3). Claws reduced, Y-shaped, of the *Xerobiotus* type (Pilato and Binda 2010) without lunulae or cuticular thickenings at the base (Fig. 4). Cuticular bars associated with claws I–III absent.

Mouth anteroventral. Buccopharyngeal apparatus of the *Macrobiotus* type (Fig. 5A), with ventral lamina and ten small peribuccal lamellae. Pharyngeal bulb spherical, with triangular apophyses, three anterior cuticular spikes (typically only two are visible in any given plane; Fig. 5C), two rod-shaped macroplacoids and a drop-shaped microplacoid (Fig. 5A). The macroplacoid length sequence is 2 < 1. The first and the second macroplacoid have a weak central and subterminal constriction, respectively (Fig. 5B–C).

Under PCM, the oral cavity armature is of the *maculatus* type, *i.e.*, with only the third band of teeth visible (Fig. 5D–G). The third band of teeth is divided into a dorsal and ventral portion. Under PCM, the dorsal teeth are composed of three distinct transverse ridges (Fig. 5D–E). The ventral teeth appear as two separate lateral transverse ridges between which one or two small medial teeth (roundish in PCM) are visible (Fig. 5F–G).

Eggs (measurements and statistics in Table 5): Eggs round, whitish and laid freely in the environment (Fig. 6A, B and G). The surface between processes is of the *hufelandi* type, *i.e.*, covered with a reticulum (Fig. 6E–F). The meshes of the reticulum are uniform in size and evenly distributed on the egg surface between the processes. Bars and nodes of the reticulum are usually thicker/wider than the meshes diameter that ranges from about 0.15 to 0.30 µm. The pillars connecting the reticulum with the chorion surface are visible only in SEM. Thickening surrounding process bases are poorly marked/visible and merge gently into the bars and nodes of the reticulum. An internal septum between the process trunk and the terminal disc is visible in PCM (Fig. 6C). Processes are of the *hufelandi* type with a concave trunk and a relatively small and concave

terminal disc. The terminal disk is greatly indented on the disk margin, creating evident teeth that have thickened and rounded tips and resemble short, nodular, finger-like apices (Fig. 5C–D). Sometimes these nodular finger-like apices are also present in the central area of the terminal disk, giving the disk a convex impression. Under SEM, the surface nodular apices/teeth in terminal discs are covered by microgranules (Fig. 6D and F).

Reproduction: The species is dioecious. Sperm with corkscrew shaped nucleus (Fig. 6H). Spermathecae present in females (Fig. 6I).

DNA sequences

DNA sequences of four markers were obtained for two individuals. Their GenBank accession numbers are:

18S: OK663219, OK663220.
28S: OK663230, OK663231.
COI: OK662990, OK662991.
ITS2: OK663208, OK663209.

DISCUSSION

Evolution of leg adaptations

Now that there are sufficient molecular and morphological data on the *Macrobiotus pseudohufelandi* complex, one can discuss potential hypotheses regarding the evolution of this group's peculiar

Table 4. Measurements [in µm] of selected morphological structures of individuals of *Macrobiotus naginae* sp. nov. mounted in Hoyer's medium

Character	N	Range		Mean		SD		Holotype	
		µm	pt	µm	pt	µm	pt	µm	pt
Body length	29	292–472	900–1209	394	1075	43	81	451	1171
Buccal tube									
Buccal tube length	30	30.3–39.9	-	36.7	-	2.3	-	38.5	-
Stylet support insertion point	30	23.2–32.1	76.4–81.0	28.6	77.9	2.0	1.2	30.9	80.3
Buccal tube external width	30	3.3–4.9	10.5–13.0	4.3	11.8	0.4	0.6	4.8	12.4
Buccal tube internal width	30	2.0–3.3	6.5–8.7	2.8	7.6	0.3	0.6	3.3	8.7
Ventral lamina length	25	18.3–25.9	53.0–69.1	22.3	61.2	1.9	3.7	23.7	61.6
Placoid lengths									
Macroplacoid 1	30	5.2–8.9	15.6–22.8	6.8	18.5	0.9	2.0	8.4	21.9
Macroplacoid 2	30	3.7–5.4	11.5–14.6	4.8	13.0	0.4	0.7	4.7	12.2
Microplacoid	30	1.3–2.7	3.7–7.0	1.8	5.0	0.4	0.8	1.9	5.0
Macroplacoid row	30	10.3–17.7	30.1–46.0	12.7	34.7	1.6	3.2	17.7	46.0
Placoid row	30	11.5–19.3	31.2–48.4	15.1	41.0	1.6	3.1	14.7	38.3
Claw I heights									
External primary branch	30	5.3–7.9	13.8–20.4	6.7	18.2	0.6	1.5	7.2	18.8
External secondary branch	27	3.8–6.1	9.8–16.0	5.1	13.8	0.7	1.6	5.6	14.5
Internal primary branch	30	4.9–7.8	12.6–20.8	6.5	17.8	0.7	1.6	7.4	19.1
Internal secondary branch	30	3.6–5.8	10.6–15.1	4.8	12.9	0.6	1.2	5.0	13.0
Claw II heights									
External primary branch	30	5.4–7.9	14.7–22.0	6.8	18.6	0.6	1.7	7.7	19.9
External secondary branch	28	3.6–6.2	9.9–16.4	5.0	13.6	0.6	1.5	4.4	11.4
Internal primary branch	28	5.0–8.2	15.4–21.4	6.8	18.6	0.7	1.6	7.4	19.2
Internal secondary branch	26	3.0–6.1	9.9–16.3	4.8	13.1	0.7	1.7	4.9	12.6
Claw III heights									
External primary branch	28	5.9–8.1	17.0–21.8	7.1	19.4	0.6	1.3	7.3	18.9
External secondary branch	26	3.5–5.7	9.4–15.5	4.7	13.0	0.6	1.5	5.7	14.7
Internal primary branch	28	5.5–7.7	16.0–21.6	6.8	18.6	0.6	1.4	7.0	18.3
Internal secondary branch	25	3.7–6.0	10.6–16.3	5.0	13.7	0.6	1.4	4.9	12.8
Claw IV heights									
Anterior primary branch	30	4.6–7.4	12.7–20.2	6.3	17.1	0.8	1.8	7.4	19.1
Anterior secondary branch	29	3.3–5.5	8.9–14.7	4.5	12.3	0.6	1.5	4.4	11.5
Posterior primary branch	30	4.6–7.4	13.8–19.7	6.3	17.2	0.7	1.5	6.5	16.8
Posterior secondary branch	29	3.2–5.7	9.1–15.1	4.7	12.7	0.7	1.7	3.9	10.2

N, number of specimens/structures measured; Range refers to the smallest and the largest structure among all measured specimens; SD, standard deviation.

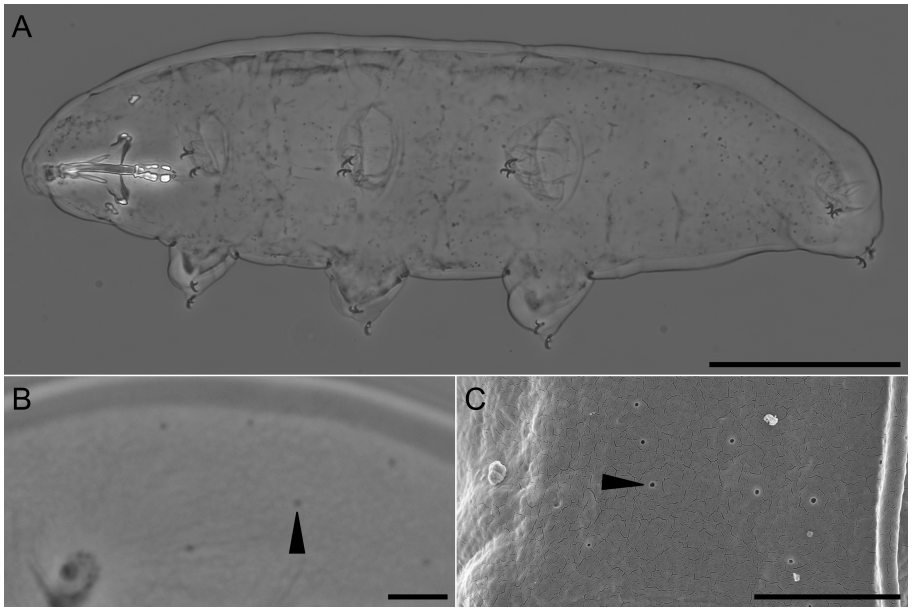

Fig. 2. *Macrobiotus naginae* sp. nov. – habitus and cuticular pores: A, dorsoventral view of the body (Holotype; Hoyer's medium, PCM); B–C, cuticular pores on the dorsal part of the body under PCM (B) and under SEM (C). Flat arrowheads indicate pores on the dorsocaudal cuticle. Scale bars: A = 100 mm; B–C = 10 mm.

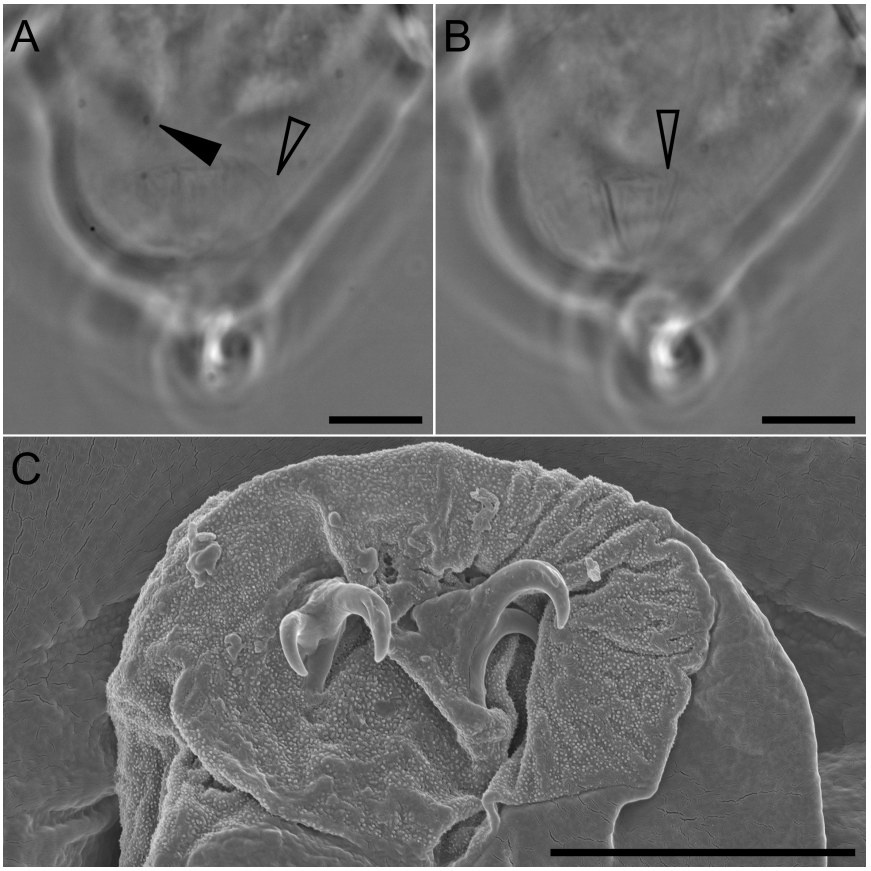

Fig. 3. *Macrobiotus naginae* sp. nov. – cuticular structures on legs: A, garter-like structure on leg II under PCM; B, garter-like structure on leg III under PCM; C, garter-like structures and claws III under SEM. Flat arrowheads indicate pores on the leg cuticle, flat empty arrowheads indicate garter-like structures. Scale bars: A–B = 20 μm; C = 10 μm.

adaptations to the soil dwelling lifestyle. Among the species for which we have molecular data, *Mac. gretae* is not only the most basal in the group, but also the one with the fewest marked claw modifications. A general trend can be observed on the phylogenetic tree of this group, with the ancestral condition being the presence of lunules on the fourth pair of legs [*Mac. gretae* (Fig. 7A) and *Mac. pseudohufelandi*], and their loss in the more derived clades, [*Mac.* gr. *pseudohufelandi* PL.360 (Fig. 7B) and *Mac. naginae*]. Unfortunately, any formal analysis of such evolutionary patterns requires sequence data for more species. Nonetheless, an approximate phylogenetic position for the remaining nominal taxa within this complex can be deduced despite lacking the genetic data associated with these species. We believe that such predictions may stimulate future hypothesis-based research on the *M. pseudohufelandi* complex. For example, *Mac. euxinus* is hypothesized to be the closest relative of *Mac. pseudohufelandi* based on morphometric and morphological similarity. Conversely, *Mac. xerophilous* lacks lunules IV and therefore could be a close relative of *Mac. naginae* sp. nov. and *Mac.* gr. *pseudohufelandi* PL.360. Lastly, *Pseudohexapodibius degenerans* (Biserov, 1990) differs from the *Mac. pseudohufelandi* complex only in its lack of claws on the fourth pair of legs. It is possible, therefore, that this species represents an even more derived branch of the *Mac. pseudohufelandi* complex and could even be assigned to *Macrobiotus*. Nevertheless, new material, preferably in the form of integrative redescription, is needed to solve this issue.

Biogeography

Until the recent record of a population *Mac. gretae* from South Africa (Stec et al. 2021 2022), the *Mac. pseudohufelandi* complex seemed to be limited to the European continent, with one exception in Tunisia (McInnes 1994). The latter highlights how biased research efforts (due mostly to the historical location of tardigrade taxonomists) influence our knowledge biogeographical patterns of tardigrades. Since most records of the species belonging to the *Mac. pseudohufelandi* complex, including the current one, are from mosses on sandy substrates (see *e.g.*, Bertolani et al. 1987; Rebecchi 1991), a comprehensive and

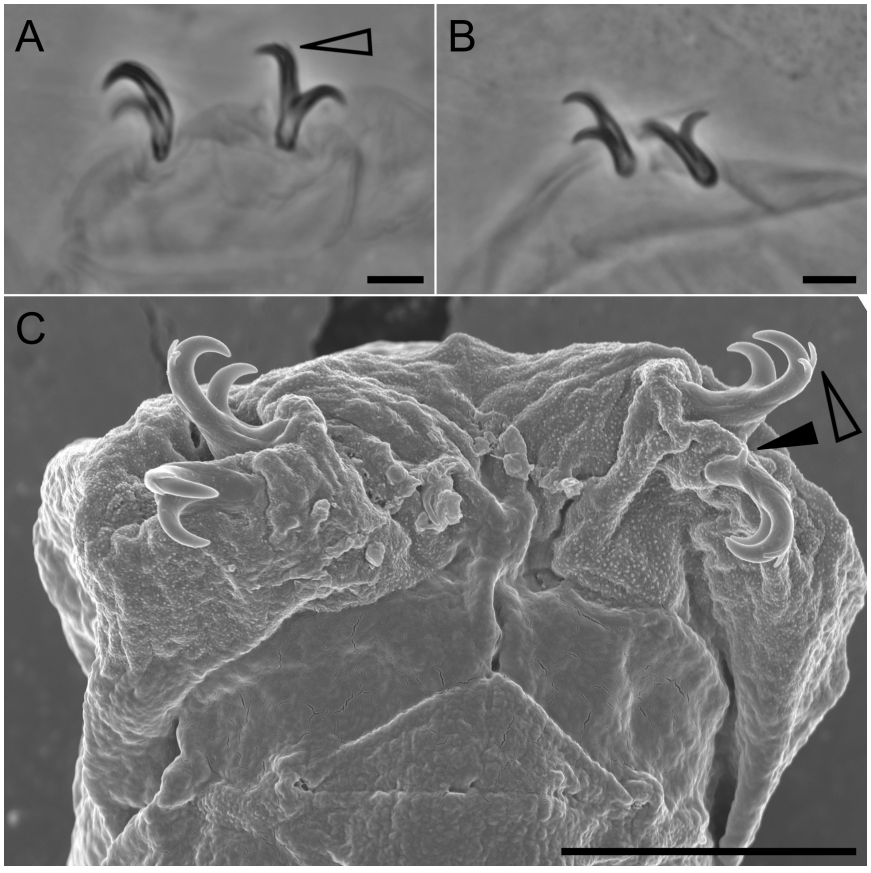

Fig. 4. *Macrobiotus naginae* sp. nov. – claws: A–B, claws I and IV, respectively, under PCM; C, claws IV under SEM. Flat arrowhead indicates an abnormal additional spur on the base on anterior claw IV; flat empty arrowheads indicate accessory points on primary branches. Scale bars = 10 μm.

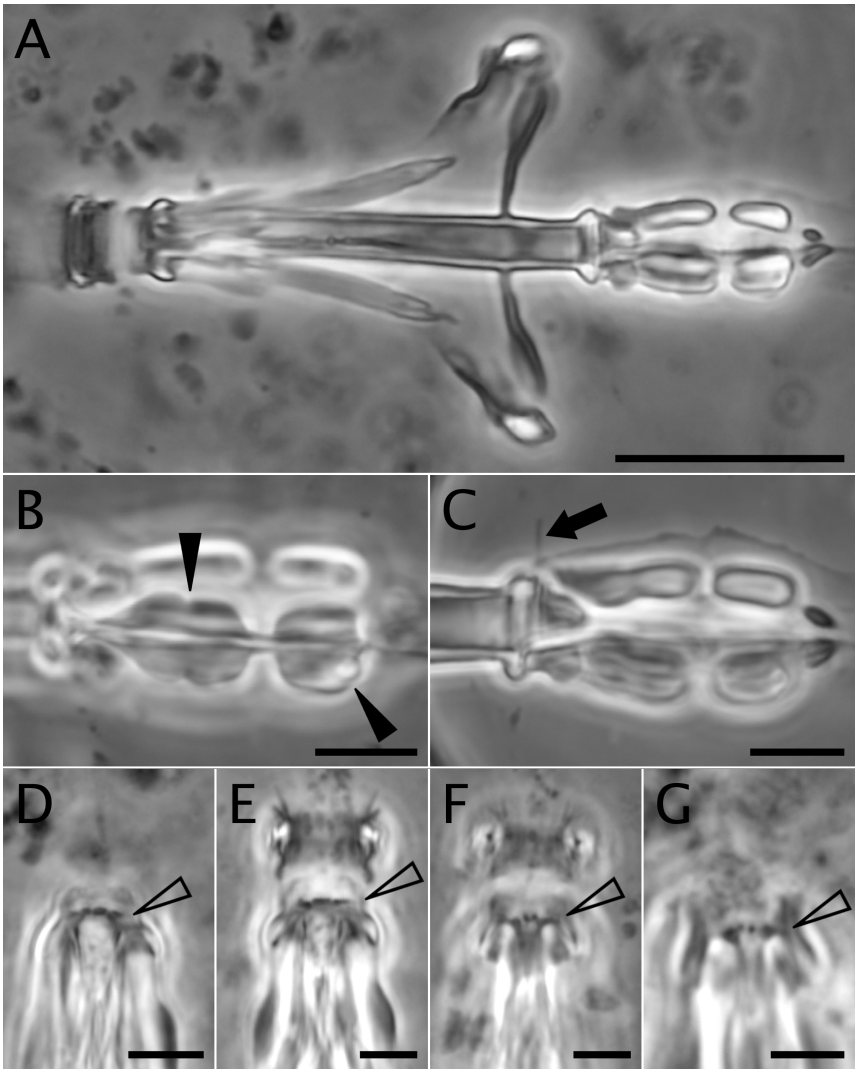

Fig. 5. *Macrobiotus naginae* sp. nov. – buccal apparatus and the oral cavity armature under PCM: A, dorsoventral view of the entire buccal apparatus; B–C, placoid morphology in ventral (B) and dorsal (C) view, respectively. D–G, oral cavity armature in dorsal (D–E) and ventral (F–G) view, respectively. Flat arrowhead indicates weak constrictions in the macroplacoids, flat empty arrowheads indicate third band of the Oral Cavity Armature (OCA), arrow indicates cuticular spikes between end of the buccal tube and anterior portion of the pharynx. Scale bars: A = 20 μm; B–G = 10 μm.

Table 5. Measurements [in μm] of selected morphological structures of eggs of *Macrobiotus naginae* sp. nov. mounted in Hoyer's medium

Character	N	Range	Mean	SD
Egg bare diameter	4	74.8–90.1	82.1	6.9
Egg full diameter	4	84.5–102.6	92.1	8.2
Process height	21	3.4–7.0	4.9	1.0
Process base width	21	4.0–8.1	5.6	1.0
Process base/height ratio	21	81%–159%	117%	18%
Terminal disc width	21	1.8–2.9	2.3	0.3
Inter-process distance	21	1.0–3.0	1.7	0.5
Number of processes on the egg circumference	4	32–38	34.0	2.8

N, number of specimens/structures measured; Range refers to the smallest and the largest structure among all measured specimens; SD, standard deviation).

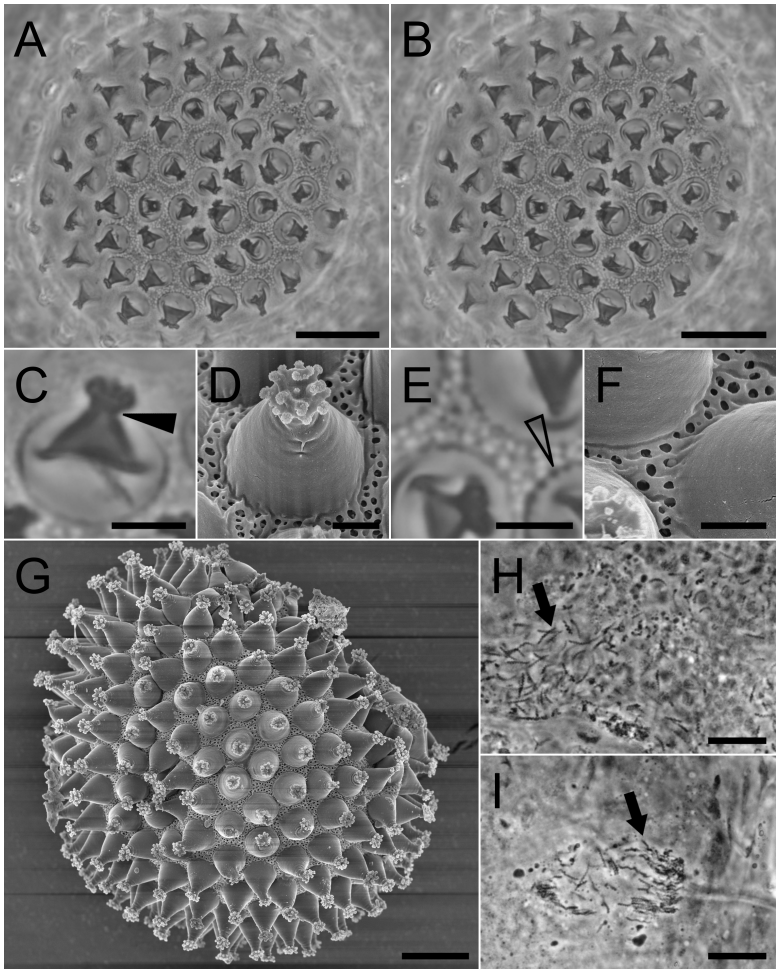

Fig. 6. *Macrobiotus naginae* sp. nov. – egg chorion morphology and reproduction: A–B, egg surface under PCM; C, egg process under PCM; D, egg process under SEM; E, chorion surface between processes under PCM; F, chorion surface between processes under SEM; G, *in toto* egg under SEM; H, orcein-stained sperm inside male gonad under PCM; H, orcein-stained sperm inside female spermatheca under PCM. Flat arrowhead indicates the septum between process trunk and terminal disk: flat empty arrowhead indicates thickenings surrounding the processes; arrows indicate sperm nuclei. Scale bars: A–B, G–I = 10 μm; C–F = 2 μm.

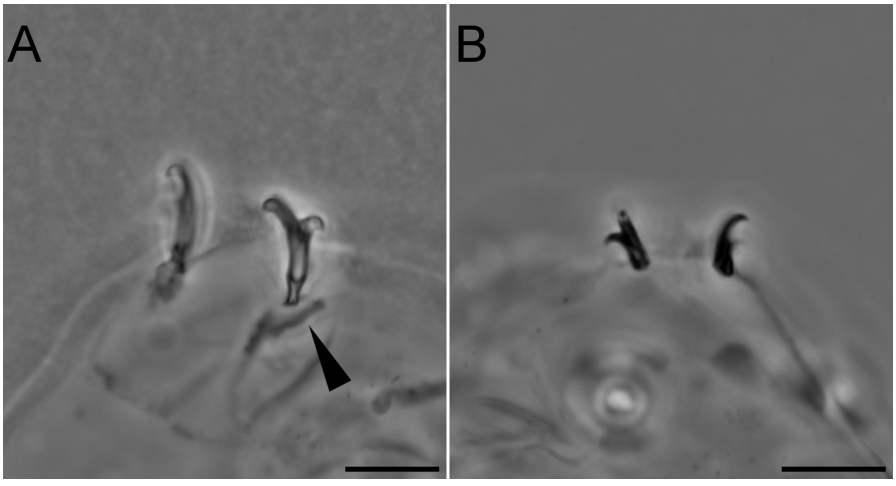

Fig. 7. Claws IV of *Macrobiotus pseudohufelandi* complex species. A, *Macrobiotus gretae* ZA.373; B, *Macrobiotus* gr. *pseudohufelandi* PL.360. Arrowhead indicates lunulae (when present). Scale bar = 20 μm.

worldwide survey of these habitats would be fruitful.

Differential diagnosis

Its reduced claws suggest that *Macrobiotus naginae* sp. nov. belongs to the *Macrobiotus pseudohufelandi* complex. However, it specifically differs from the other species of this group:

Macrobiotus gretae (Massa, Guidetti, Cesari, Rebecchi and Jönsson, 2021) by lacking cuticular bars and lunulae under claws IV (present in *M. gretae*) and by the reticulate (*hufelandi* type) egg chorion (wrinkled (*persimilis* type) in *M. gretae*).

Macrobiotus euxinus (Pilato, Kiosya, Lisi, Inshina and Biserov, 2011) by lacking lunules on the hind legs (present in *M. euxinus*) and by having the dorsal band of the posterior OCA band formed by three distinct crests (joined together forming a continuous arc in *M. euxinus*).

Macrobiotus pseudohufelandi Iharos, 1966 by lacking lunules on the hind legs (present in *M. pseudohufelandi*).

Macrobiotus xerophilus (Dastych, 1978) by having the dorsal band of the posterior OCA band formed by three distinct crests (joined together forming a continuous arc in *M. xerophilus*) and by the having the egg processes of the *hufelandi* type (hemispherical in *M. xerophilus*).

Dichotomous key to the *Macrobiotus pseudohufelandi* complex

1. Lunulae under claws IV present 2
– Lunulae under claws IV absent 4
2(1) Cuticular pores visible in LM, bars under claws IV present ..... *Macrobiotus gretae* (Massa, Guidetti, Cesari, Rebecchi & Jönsson, 2021)
– Cuticular pores not visible in LM, bars under claws IV absent 3
3(2) Buccal tube width *pt* < 12% and the stylet support insertion point *pt* < 78% .... *Macrobiotus euxinus* (Pilato, Kiosya, Lisi, Inshina & Biserov, 2011)
– Buccal tube width *pt* >15% and the stylet support insertion point *pt* > 79% ..... *Macrobiotus pseudohufelandi* Iharos, 1966
4(1) Posterior OCA band formed by three distinct crests, egg processes *hufelandi* type .....*Macrobiotus naginae* sp. nov.
– Posterior OCA band formed by a continuous arc; egg processes hemispherical ..... *Macrobiotus xerophilous* (Dastych, 1978)

CONCLUSIONS

This contribution raises the number of formally described species attributed to the *Macrobiotus pseudohufelandi* complex to five. The presentation of a dichotomous key to this complex will facilitate future studies on those taxa. Furthermore, the presence of *Macrobiotus naginae* in association with inland sand dunes illustrates the importance of this ecosystem to peculiar meiofauna taxa that have clearly developed adaptations—such as reduced claws and legs—and highlights the importance of protecting these unique habitats. The phylogenetic position among *Macrobiotus* and monophyly of the *Macrobiotus pseudohufelandi* complex have been confirmed. The hypotheses regarding the evolution of soil adaptations in the group are presented with the objective to stimulate new hypothesis-driven research.

List of abbreviations

18S, 18S Ribosomal RNA.
28S, 28S Ribosomal RNA.
ABGD, Automatic Barcode Gap Discovery.
COI, Cytochrome Oxidase I.
ITS2, Internal Transcribed Spacer 2.
OCA, Oral Cavity Armature.
PCM, Phase Contrast Microscopy.
SEM, Scanning Electron Microscopy.

Acknowledgments: This work and the new species name were registered with ZooBank under urn:lsid:zoobank.org:pub:80C8AC73-ABAC-4612-A990-75435963986C. Sampling was performed under sampling permit MH1072/2020 issued by Metsähallitus Forststyrelsen (Finland) to MV. We thank Witold Morek (Jagellonian University, Poland) for providing photographs of *Macrobiotus* gr. *pseudohufelandi* Pl.360 and *Macrobiotus gretae* ZA.373. The study was supported by the Academy of Finland Fellowship (grant no. 314219 and 335759 to SC) and the *Preludium* programme of the Polish National Science Centre (grant no. 2018/31/N/NZ8/03096 to DS). During this study, DS was supported by the Foundation for Polish Science (FNP). We thank Alex Groke and Claudio Ferrari for providing samples used in this study.

Authors' contributions: MV, DS and SC conceived the study. MV, JC, SR, SC performed sampling and extracted the animals and eggs. MV and DS collected morphological data. TV and SR collected morphometric data. DS collected molecular data. MV and DS analysed morphological, morphometric, and molecular data. MV drafted the manuscript. All the authors read and approved the final manuscript.

Competing interests: The authors declare that they have no competing interests.

Availability of data and materials: The slides and SEM stubs are deposited at the department of Biological and Environmental Sciences, University of Jyväskylä, Survontie 9C, 40500 Jyväskylä, Finland. DNA sequences produced in this study are deposited in GenBank (see main text for accession numbers) and morphometric measurements of *Macrobiotus naginae* sp. nov. are provided in Excel format as a supplementary file to this article.

Consent for publication: Not applicable.

Ethics approval consent to participate: Not applicable.

REFERENCES

Aartolahti T. 1973. Morphology, vegetation and development of Rokuanvaara, an esker and dune complex in Finland. Fennia - International Journal of Geography **127:**1.

Astrin JJ, Stüben PE. 2008. Phylogeny in cryptic weevils: molecules, morphology and new genera of western Palaearctic Cryptorhynchinae (Coleoptera: Curculionidae). Invertebr Syst **22:**503–522. doi:10.1071/IS07057.

Bah T. 2011. Inkscape: guide to a vector drawing program. Upper Saddle River, NJ, USA.

Bertolani R. 1971. Contributo alla cariologia dei Tardigradi. Osservazioni su *Macrobiotus hufelandii*. Rend Lincei-Mat Appl **50:**772–775.

Bertolani R, Biserov VI. 1996. Leg and claw adaptations in soil tardigrades, with erection of two new genera of Eutardigrada, Macrobiotidae: *Pseudohexapodibius* and *Xerobiotus*. Invertebr Biol **115:**299–304. doi:10.2307/3227019.

Bertolani R, Garagna S, Manicardi GC, Redi CA. 1987. *Macrobiotus pseudohufelandi* Iharos as a model for cytotaxonomic study in populations of eutardigrades (Tardigrada). Experientia **43:**210–213. doi:10.1080/00087114.1991.10797195.

Bertolani R, Guidetti R, Marchioro T, Altiero T, Rebecchi L, Cesari M. 2014. Phylogeny of Eutardigrada: New molecular data and their morphological support lead to the identification of new evolutionary lineages. Mol Phylogenet and Evol **76:**110–126. doi:10.1016/j.ympev.2014.03.006.

Casquet J, Thebaud C, Gillespie RG. 2012. Chelex without boiling, a rapid and easy technique to obtain stable amplifiable DNA from small amounts of ethanol-stored spiders. Mol Ecol Resour **12:**136–141. doi:10.1111/j.1755-0998.2011.03073.x.

Czerneková M, Jönsson KI, Hajer J, Devetter M. 2018. Evaluation of extraction methods for quantitative analysis of tardigrade populations in soil and leaf litter. Pedobiologia **70:**1–5. doi:10.1016/j.pedobi.2018.06.005.

Dastych H. 1978. *Parhexapodibius xerophilus* sp. nov., a new species of Tardigrada from Poland. Bull Acad Polon Sci **26:**479–481.

Dastych H. 1980. Niesporczaki (Tardigrada) Tatrzańskiego Parku Narodowego. Monografie Fauny Polski. Polish Academy of Sciences, Krakow, Poland.

Doyère ML. 1840. Memorie sur les Tardigrades. Annales des Sciences Naturelles. Zoologie **14:**269–362.

Edgar R. 2004. MUSCLE: multiple sequence alignment with high accuracy and high throughput. Nucleic Acids Res **32:**1792–1797. doi:10.1093/nar/gkh340.

From S. 2005. Paahdeympäristöjen ekologia ja uhanalaiset lajit. Suomen ympäristö 774. (in Finnish with an English summary: the ecology and threatened species of sunny and dry habitats)

Gąsiorek P, Stec D, Zawierucha K, Kristensen RM, Michalczyk Ł. 2018. Revision of *Testechiniscus* Kristensen, 1987 (Heterotardigrada: Echiniscidae) refutes the polar-temperate distribution of the genus. Zootaxa **4472:**261–297. doi:10.11646/zootaxa.4472.2.3.

Iharos G. 1966. Beitrage zur Kenntnis der Tardigraden-Fauna Osterreichs. Acta Zool Acad Sci Hung **12:**123.

Jalas J. 1953. Rokua: suunnitellun kansallispuiston kasvillisuus ja kasvisto. Silva Fennica 81. Suomen metsätieteellinen seura.

Kaczmarek Ł, Cytan J, Zawierucha K, Diduszko D, Michalczyk Ł. 2014. Tardigrades from Peru (South America), with descriptions of three new species of Parachela. Zootaxa **3790:**357–379. doi:10.11646/zootaxa.3790.2.5.

Kaczmarek Ł, Michalczyk Ł. 2017. The *Macrobiotus hufelandi* group (Tardigrada) revisited. Zootaxa **4363:**101–123. doi:10.11646/zootaxa.4363.1.4.

Katoh K, Misawa K, Kuma K, Miyata T. 2002. MAFFT: A novel method for rapid multiple sequence alignment based on fast Fourier transform. Nucleic Acids Res **30:**3059–3066. doi:10.1093/nar/gkf436.

Katoh K, Toh H. 2008. Recent developments in the MAFFT multiple sequence alignment program. Brief Bioinform **9:**286–298. doi:10.1093/bib/bbn013.

Kiosya Y, Pogwizd J, Matsko Y, Vecchi M, Stec D. 2021. Phylogenetic position of two *Macrobiotus* species with a revisional note on *Macrobiotus sottilei* Pilato, Kiosya, Lisi & Sabella, 2012 (Tardigrada: Eutardigrada: Macrobiotidae). Zootaxa **4933:**113–135. doi:10.11646/zootaxa.4933.1.5.

Kontula T, Raunio A. 2018. Suomen luontotyyppien uhanalaisuus 2018: Luontotyyppien punainen kirja. Osa 2: Luontotyyppien kuvaukset.

Kumar S, Stecher G, Tamura K. 2016. MEGA7: molecular evolutionary genetics analysis version 7.0 for bigger datasets. Mol Biol Evol **33:**1870–1874. doi:10.1093/molbev/msw054.

Lanfear R, Frandsen PB, Wright AM, Senfeld T, Calcott B. 2016. PartitionFinder 2: new methods for selecting partitioned models of evolution for molecular and morphological phylogenetic analyses. Mol Biol Evol **34:**772–773. doi:10.1093/molbev/msw260.

Marley NJ, McInnes SJ, Sands CJ. 2011. Phylum Tardigrada: a re-evaluation of the Parachela. Zootaxa **2819:**51–64. doi:10.11646/zootaxa.2819.1.2.

Massa E, Guidetti R, Cesari M, Rebecchi L, Jönsson KI. 2021. Tardigrades of Kristianstads Vattenrike Biosphere Reserve with description of four new species from Sweden. Sci Rep **11:**1–19. doi:10.1038/s41598-021-83627-w.

McInnes SJ. 1994. Zoogeographic distribution of terrestrial/freshwater tardigrades from current literature. J Nat Hist **28:**257–352.

Michalczyk Ł, Kaczmarek Ł. 2003. A description of the new tardigrade *Macrobiotus reinhardti* (Eutardigrada: Macrobiotidae, *harmsworthi* group) with some remarks on the oral cavity armature within the genus *Macrobiotus* Schultze. Zootaxa **331:**1–24. doi:10.11646/zootaxa.331.1.1.

Michalczyk Ł, Kaczmarek Ł. 2013. The Tardigrada Register: a comprehensive online data repository for tardigrade taxonomy. J Limnol **72(s1):**175–181. doi:10.4081/jlimnol.2013.s1.e22.

Miller MA, Pfeiffer W Schwartz T. 2010. Creating the CIPRES Science Gateway for inference of large phylogenetic trees. 2010 gateway computing environments workshop (GCE), pp. 1–8. doi:10.1109/GCE.2010.5676129.

Mironov SV, Dabert J, Dabert M. 2012. A new feather mite species of the genus *Proctophyllodes* Robin, 1877 (Astigmata:

Proctophyllodidae) from the Long-tailed Tit *Aegithalos caudatus* (Passeriformes: Aegithalidae): morphological description with DNA barcode data. Zootaxa **3253:**54–61. doi:10.11646/zootaxa.3253.1.2.

Morek W, Stec D, Gąsiorek P, Schill RO, Kaczmarek Ł, Michalczyk Ł. 2016. An experimental test of eutardigrade preparation methods for light microscopy. Zool J Linnean Soc **178:**785–793. doi:10.1111/zoj.12457.

Mutterer J, Zinck E. 2013. Quick-and-clean article Figures with FigureJ. J Micros **252:**89–91. doi:10.1111/jmi.12069.

Pilato G. 1981. Analisi di nuovi caratteri nello studio degli Eutardigradi. Animalia **8:**51–57.

Pilato G, Binda MG. 2010. Definition of families, subfamilies, genera and subgenera of the Eutardigrada, and keys to their identification. Zootaxa **2404:**1–54. doi:10.5281/zenodo.194138.

Pilato G, Kiosya Y, Lisi O, Inshina V, Biserov V. 2011. Annotated list of Tardigrada records from Ukraine with the description of three new species. Zootaxa **3123:**1–31. doi:10.11646/zootaxa.3123.1.1.

Puillandre N, Lambert A, Brouillet S, Achaz GJME. 2012. ABGD, Automatic Barcode Gap Discovery for primary species delimitation. Mol Ecol **21:**1864–1877. doi:10.1111/j.1365-294x.2011.05239.x.

Rambaut A. 2007. FigTree, a graphical viewer of phylogenetic trees Available at: http://tree.bio.ed.ac.uk/software/figtree/.

Rambaut A, Drummond A, Xie D, Baele G, Suchard M. 2018. Posterior summarization in Bayesian phylogenetics using Tracer 1.7. Syst Biol **67:**901–904. doi:10.1093/sysbio/syy032.

Rebecchi L. 1991. Karyological analysis on *Macrobiotus pseudohufelandi* (Tardigrada, Macrobiotidae) and a new finding of a tetraploid population. Caryologia **44:**301–307. doi:10.1080/00087114.1991.10797195.

Rebecchi L. 1997. Ultrastructural study of spermiogenesis and the testicular and spermathecal spermatozoon of the gonochoristic tardigrade *Xerobiotus pseudohufelandi* (Eutardigrada, Macrobiotidae). J Morphol **234:**11–24. doi:10.1002/(sici)1097-4687(199710)234:1%3C11::aid-jmor2%3E3.0.co;2-q.

Richters F. 1926. Tardigrada. *In*: Kükenthal, W. & Krumbach, T. (Eds.). Handbuch der Zoologie **3:**58–61.

Ronquist F, Teslenko M, van der Mark P, Ayres D, Darling A, Höhna S, Larget B, Liu L, Suchard M, Huelsenbeck J. 2012. MrBayes 3.2: efficient Bayesian phylogenetic inference and model choice across a large model space. Syst Biol **61:**539–542. doi:10.1093/sysbio/sys029.

Roszkowska M, Gołdyn B, Wojciechowska D, Kosicki JZ, Fiałkowska E, Kmita H, Kaczmarek Ł. 2021. Tolerance to anhydrobiotic conditions among two coexisting tardigrade species differing in life strategies. Zool Stud **60:**74. doi:10.6620/ZS.2021.60-74.

Sarala P, Johansson P, Lunkka JP. 2006. Late Pleistocene glacigenic deposits in the central part of the Scandinavian ice sheet: Excursion guide. The INQUA Peribaltic Group Field Symposium in Finland, September 11–15, 2006. Geological Survey of Finland, Rovaniemi, pp. 24.

Schultze CAS. 1834. *Macrobiotus Hufelandii* animal e crustaceorum classe novum, reviviscendi post diuturnam asphixiam et aridiatem potens. C. Curths, Berlin, Germany.

Schuster RO, Nelson DR, Grigarick AA, Christenberry D. 1980. Systematic criteria of the Eutardigrada. Trans Am Microsc Soc **99:**284–303. doi:10.2307/3226004.

Stec D, Dudziak M, Michalczyk Ł. 2020a. Integrative descriptions of two new Macrobiotidae species (Tardigrada: Eutardigrada: Macrobiotoidea) from French Guiana and Malaysian Borneo. Zool Stud **59:**23. doi:10.6620/ZS.2020.59-23.

Stec D, Gąsiorek P, Morek W, Kosztyła P, Zawierucha K, Michno K, Kaczmarek Ł, Prokop ZM, Michalczyk Ł. 2016. Estimating optimal sample size for tardigrade morphometry. Zool J Linnean Soc **178:**776–784. doi:10.1111/zoj.12404.

Stec D, Kristensen RM, Michalczyk Ł. 2020b. An integrative description of *Minibiotus ioculator* sp. nov. from the Republic of South Africa with notes on *Minibiotus pentannulatus* Londoño et al. 2017 (Tardigrada: Macrobiotidae). Zool Anz **286:**117–134. doi:10.1016/j.jcz.2020.03.007.

Stec D, Morek W, Gąsiorek P, Michalczyk Ł. 2018. Unmasking hidden species diversity within the *Ramazzottius oberhaeuseri* complex, with an integrative redescription of the nominal species for the family Ramazzottiidae (Tardigrada: Eutardigrada: Parachela). Syst and Biodivers **16:**357–376. doi:10.1080/14772000.2018.1424267.

Stec D, Smolak R, Kaczmarek Ł, Michalczyk Ł. 2015. An integrative description of *Macrobiotus paulinae* sp. nov. (Tardigrada: Eutardigrada: Macrobiotidae: *hufelandi* group) from Kenya. Zootaxa **4052:**501–526. doi:10.11646/zootaxa.4052.5.1.

Stec D, Vecchi M, Calhim S, Michalczyk Ł. 2021. New multilocus phylogeny reorganises the family Macrobiotidae (Eutardigrada) and unveils complex morphological evolution of the *Macrobiotus hufelandi* group. Mol Phylogenet and Evol **160:**106987. doi:10.1016/j.ympev.2020.106987.

Stec D, Vončina K, Kristensen RM, Michalczyk Ł. 2022. The *Macrobiotus ariekammensis* species complex provides evidence for parallel evolution of claw elongation in macrobiotid tardigrades. Zool J Linnean Soc, zlab 101. doi:10.1093/zoolinnean/zlab101.

Stec D, Zawierucha K, Michalczyk Ł. 2017. An integrative description of *Ramazzottius subanomalus* (Biserov, 1985) (Tardigrada) from Poland. Zootaxa **4300:**403–420. doi:10.11646/zootaxa.4300.3.4.

Thulin G. 1928. Über die Phylogenie und das System der Tardigraden. Hereditas **11:**207–266.

Vecchi M, Bruneaux M. 2021. Concatipede: an R package to concatenate fasta sequences easily. doi:10.5281/zenodo.5130604.

Vecchi M, Stec D. 2021. Integrative descriptions of two new *Macrobiotus* species (Tardigrada, Eutardigrada, Macrobiotidae) from Mississippi (USA) and Crete (Greece). Zoosystematics Evol **97:**281–306. doi:10.3897/zse.97.65280.

Villani MG, Allee LL, Diaz A, Robbins PS. 1999. Adaptive strategies of edaphic arthropods. Annu Rev Entomol **44:**233–256. doi:10.1146/annurev.ento.44.1.233.

Supplementary materials

Table S1. Raw morphometric data for *Macrobiotus naginae* sp. nov. from Finland. (download)

Table S2. Additional Macrobiotidae populations sequenced for phylogenetic reconstruction. (download)

Table S3. Accession numbers of sequences downloaded from GenBank for phylogenetic reconstruction. (download)

Appendix 1. 18S reference alignment. (download)

Appendix 2. 28S reference alignment. (download)

Appendix 3. PartitionFinder model selection analysis results. (download)

Appendix 4. MrBayes analysis input file with alignment. (download)

Appendix 5. Complete output tree from MrBayes analysis. (download)

Appendix 6. ABGD species delimitation results. (download)